

Implicit handling of multilayered material substrates in full-wave SCUFF-EM calculations

Homer Reid

August 16, 2017

Contents

1	Overview	2
2	Evaluation of substrate Green's-function correction	4
2.1	Derivation of momentum-space DGF, take 1: Effective surface-current picture	5
2.2	Derivation of momentum-space DGF, take 2: Plane-wave (Fresnel) scattering picture)	12
2.2.1	Plane-wave decomposition of point-source fields	13
2.2.2	Plane-wave decomposition of DGFs	15
3	Plane-wave reflection coefficients for layered material substrates	17
3.1	Reflection coefficients for a single material interface	17
3.2	Reflection coefficients for multilayer substrates	17
4	Alternative approach to evaluating RWG integrals	18
5	Evaluation of q integrals	19

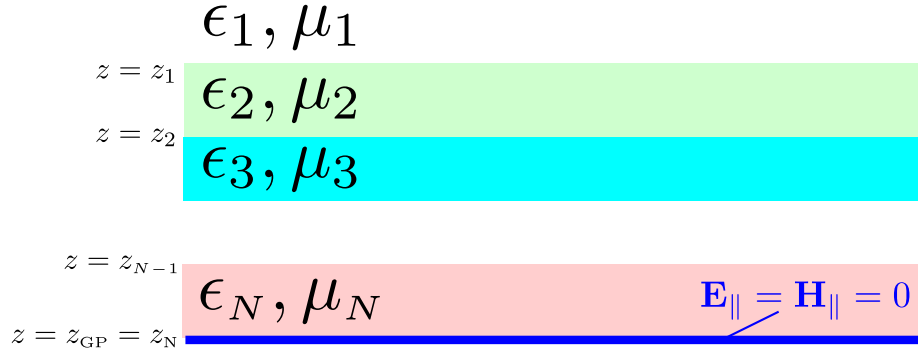


Figure 1: Geometry of the layered substrate. The n th layer has relative permittivity and permeability ϵ_n, μ_n , and its lower surface lies at $z = z_n$. The ground plane, if present, lies at $z = z_{GP}$.

1 Overview

In a previous memo¹ I considered SCUFF-STATIC electrostatics calculations in the presence of a multilayered dielectric substrate. In this memo I extend that discussion to the case of *full-wave* (i.e. nonzero frequencies beyond the quasisstatic regime) scattering calculations in the SCUFF-EM core library.

Substrate geometry

As shown in Figure 1, I consider a multilayered substrate consisting of N material layers possibly terminated by a perfectly-conducting ground plane. The uppermost layer (layer 1) is the infinite half-space above the substrate. The n th layer has relative permittivity and permeability ϵ_n, μ_n , and its lower surface lies at $z = z_n$. The ground plane, if present, lies at $z \equiv z_N \equiv z_{GP}$. If the ground plane is absent, layer N is an infinite half-space² ($z_N = -\infty$).

Mechanics of implementation in SCUFF-EM

The mechanics of implementing support for multilayer substrates in SCUFF-EM boils down to a two-step process:

- Devise a numerical scheme for computing the substrate contribution $\mathcal{G}^{\text{subs}}$ to the full dyadic Green's function (DGF) $\mathcal{G} \equiv \mathcal{G}^0 + \mathcal{G}^{\text{subs}}$. The quantity $\mathcal{G}(\mathbf{x}, \mathbf{x}')$ describes the fields at \mathbf{x} due to point sources at \mathbf{x}' , including both the direct contributions that are present in the absence of the substrate (\mathcal{G}^0) and the contributions due to scattering from the substrate ($\mathcal{G}^{\text{subs}}$).

¹“Implicit handling of multilayered dielectric substrates in SCUFF-STATIC”

²As in the electrostatic case, this means that a finite-thickness substrate consisting of N material layers is described as a stack of $N + 1$ layers in which the bottommost layer is an infinite vacuum half-space.

- Incorporate the substrate DGF correction $\mathcal{G}^{\text{subs}}$ into the existing SCUFF-EM framework for evaluating 4-dimensional integrals of the form $\langle \mathbf{b}_\alpha | \mathcal{G} | \mathbf{b}_\beta \rangle$ where $\mathbf{b}_{\alpha,\beta}$ are RWG basis functions. To achieve reasonable efficiency, this will require combining a variety of numerical computational techniques, including look-up tables, interpolation schemes, and asymptotic expansions.

In this memo I will discuss methods for attacking both of these challenges.

2 Evaluation of substrate Green's-function correction

My calculation of $\mathcal{G}^{\text{subs}}$ proceeds in two stages:

- Obtain expressions for the 2D Fourier transform of the substrate GF correction, $\tilde{\mathcal{G}}^{\text{subs}}(\mathbf{q})$. I consider two separate ways of doing this:
 - By using surface-integral-equation methods to solve a scattering problem to determine effective surface-current densities induced on material interfaces by radiating point sources (Section 2.1).
 - By resolving the fields radiated by point sources into superpositions of plane waves, then considering the reflection of each individual plane wave from the multilayer substrate (Section 2.2).
- Evaluate the 2D integrals over the \mathbf{q} variable to effect the inverse Fourier transform from momentum space to real space, $\tilde{\mathcal{G}}^{\text{subs}}(\mathbf{q}) \rightarrow \mathcal{G}^{\text{subs}}(\boldsymbol{\rho})$. This calculation proceeds in two stages:
 - Use the known structure of $\tilde{\mathcal{G}}(\mathbf{q})$ to reduce 2D integrals over \mathbf{q} to 1D integrals over $q = |\mathbf{q}|$ (Section ??).
 - Devise numerical quadrature methods for evaluating the q integrals, including efficient and accurate handling of integrable singularities and undamped oscillatory integrands (Section ??).

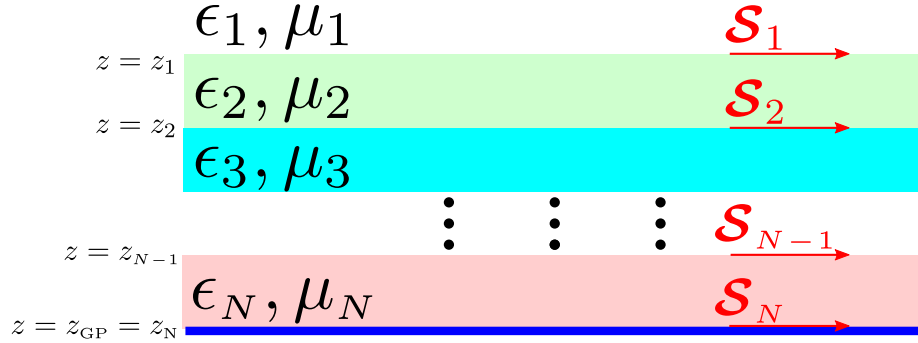


Figure 2: Effective surface-current approach to treatment of multilayer substrate. External field sources induce a distribution of electric and magnetic surface currents $\mathcal{S}_n = \begin{pmatrix} \mathbf{K}_n \\ \mathbf{N}_n \end{pmatrix}$ on the n th material interface, and the fields radiated by these effective currents account for the disturbance presented by the substrate.

2.1 Derivation of momentum-space DGF, take 1: Effective surface-current picture

An alternative way to account for the disturbance produced by the substrate is to consider the effective tangential electric and magnetic surface currents \mathbf{K} and \mathbf{N} induced on the interfacial layers by the external field sources (Figure 2). This is the direct extension to full-wave problems of the formalism I used in the electrostatic case, and it comports well with the spirit of surface-integral-equation methods.

More specifically, on the material interface layer at $z = z_n$ I have a four-vector surface-current density $\mathcal{S}_n(\boldsymbol{\rho})$, where $\boldsymbol{\rho} = (x, y)$ and the components of \mathcal{S} are

$$\mathcal{S}_n(\boldsymbol{\rho}) = \begin{pmatrix} K_x(\boldsymbol{\rho}) \\ K_y(\boldsymbol{\rho}) \\ N_x(\boldsymbol{\rho}) \\ N_y(\boldsymbol{\rho}) \end{pmatrix}. \quad (1)$$

Fields in layer interiors. I will adopt the convention that the lower (upper) bounding surface for each region is the positive (negative) bounding surface for that region in the usual sense of SCUFF-EM regions and surfaces (in which the sign of a {surface, region} pair $\{\mathcal{S}, \mathcal{R}\}$ is the sign with which surface currents on \mathcal{S} contribute to fields in \mathcal{R}). Thus, at a point $\mathbf{x} = (\boldsymbol{\rho}, z)$ in the interior of layer n ($z_{n-1} > z > z_n$), the six-vector of total fields $\mathcal{F} = \begin{pmatrix} \mathbf{E} \\ \mathbf{H} \end{pmatrix}$ reads

$$\mathcal{F}_n(\boldsymbol{\rho}, z) = -\mathcal{G}^n(z_{n-1}) \star \mathcal{S}_{n-1} + \mathcal{G}^n(z_n) \star \mathcal{S}_n + \mathcal{F}_n^{\text{ext}}(\boldsymbol{\rho}, z) \quad (2)$$

where $\mathcal{F}_n^{\text{ext}}$ are the externally-sourced (incident) fields due to sources in layer n , \mathcal{G}^n is the homogeneous dyadic Green's function for material layer n , and \star is shorthand for the convolution operation

$$“\mathcal{F}(\boldsymbol{\rho}, z) \equiv \mathcal{G}(z') \star \mathcal{S}'' \implies \mathcal{F}(\boldsymbol{\rho}, z) = \int \mathcal{G}(\boldsymbol{\rho} - \boldsymbol{\rho}', z - z') \cdot \mathcal{S}(\boldsymbol{\rho}') d\boldsymbol{\rho}' \quad (3)$$

where the integral extends over the entire interfacial plane. I will evaluate convolutions of this form using the 2D Fourier representation of \mathcal{G} :

$$\mathcal{G}^n(\boldsymbol{\rho}, z) = \int \frac{d^2\mathbf{q}}{(2\pi)^2} \widetilde{\mathcal{G}}^n(\mathbf{q}, z) e^{i\mathbf{q} \cdot \boldsymbol{\rho}} \quad (4a)$$

$$\widetilde{\mathcal{G}}^n(\mathbf{q}, z) = \frac{1}{2} \begin{pmatrix} -\frac{\omega\mu_0\mu_n}{q_{zn}} \widetilde{\mathbf{G}}^\pm & +\widetilde{\mathbf{C}}^\pm \\ -\widetilde{\mathbf{C}}^\pm & -\frac{\omega\epsilon_0\epsilon_n}{q_{zn}} \widetilde{\mathbf{G}}^\pm \end{pmatrix} e^{iq_z|z|} \quad (4b)$$

$$\widetilde{\mathbf{G}}^\pm(\mathbf{q}, k) = \begin{pmatrix} 1 & 0 & 0 \\ 0 & 1 & 0 \\ 0 & 0 & 1 \end{pmatrix} - \frac{1}{k^2} \begin{pmatrix} q_x^2 & q_x q_y & \pm q_x q_z \\ q_y q_x & q_y^2 & \pm q_y q_z \\ \pm q_z q_x & \pm q_z q_y & q_z^2 \end{pmatrix} \quad (4c)$$

$$\widetilde{\mathbf{C}}^\pm(\mathbf{q}, k) = \begin{pmatrix} 0 & \mp 1 & +q_y/q_z \\ \pm 1 & 0 & -q_x/q_z \\ -q_y/q_z & +q_x/q_z & 0 \end{pmatrix} \quad (4d)$$

$$k_n \equiv \sqrt{\epsilon_0\epsilon_n\mu_0\mu_n} \cdot \omega, \quad q_z \equiv \sqrt{k^2 - |\mathbf{q}|^2}, \quad \pm = \text{sign } z. \quad (4e)$$

With this representation, convolutions like (3) become products in Fourier space:

$$\mathcal{G}(z') \star \mathcal{S} = \mathcal{F}(\boldsymbol{\rho}, z) = \int \frac{d^2\mathbf{q}}{(2\pi)^2} \widetilde{\mathcal{F}}(\mathbf{q}, z) e^{i\mathbf{q} \cdot \boldsymbol{\rho}}, \quad \text{with } \widetilde{\mathcal{F}}(\mathbf{q}, z) = \widetilde{\mathcal{G}}(\mathbf{q}, z - z') \widetilde{\mathcal{S}}(\mathbf{q})$$

Surface currents from incident fields. To determine the surface currents induced by given incident-field sources, I apply boundary conditions. The boundary condition at $z = z_n$ is that the tangential \mathbf{E}, \mathbf{H} fields be continuous: in Fourier space, we have

$$\widetilde{\mathcal{F}}_\parallel(\mathbf{q}, z = z_n^+) = \widetilde{\mathcal{F}}_\parallel(\mathbf{q}, z = z_n^-) \quad (5)$$

The fields just **above** the interface ($z \rightarrow z_n^+$) receive contributions from three sources:

- Surface currents at $z = z_{n-1}$, which contribute with a minus sign and via the Green's function for region n ;
- Surface currents at $z = z_n$, which contribute with a plus sign and via the Green's function for region n ; and

- external field sources in region n .

The fields just **below** the interface ($z = z_n^-$) receive contributions from three sources:

- Surface currents at $z = z_n$, which contribute with a minus sign and via the Green's function for region $n + 1$;
- Surface currents at $z = z_{n+1}$, which contribute with a plus sign and via the Green's function for region $n + 1$; and
- external field sources in region $n + 1$.

Then equation (5) reads

$$\begin{aligned} & -\widetilde{\mathcal{G}}_{\parallel}^n(z_n - z_{n-1}) \cdot \widetilde{\mathcal{S}}_{n-1} + \widetilde{\mathcal{G}}_{\parallel}^n(0^+) \cdot \widetilde{\mathcal{S}}_n + \widetilde{\mathcal{F}}_{n\parallel}^{\text{ext}}(z_n) \\ & = -\widetilde{\mathcal{G}}_{\parallel}^{n+1}(0^-) \cdot \widetilde{\mathcal{S}}_n + \widetilde{\mathcal{G}}_{\parallel}^{n+1}(z_n - z_{n+1}) \cdot \widetilde{\mathcal{S}}_{n+1} + \widetilde{\mathcal{F}}_{n+1\parallel}^{\text{ext}}(z_n) \end{aligned}$$

or

$$\mathbf{M}_{n,n-1} \cdot \widetilde{\mathcal{S}}_{n-1} + \mathbf{M}_{n,n} \cdot \widetilde{\mathcal{S}}_n + \mathbf{M}_{n,n+1} \cdot \widetilde{\mathcal{S}}_{n+1} = \widetilde{\mathcal{F}}_{n+1\parallel}^{\text{ext}}(z_n) - \widetilde{\mathcal{F}}_{n\parallel}^{\text{ext}}(z_n) \quad (6)$$

with the 4×4 matrix blocks³

$$\mathbf{M}_{n,n-1} = -\widetilde{\mathcal{G}}_{\parallel}^n(z_n - z_{n-1}) \quad (9a)$$

$$\mathbf{M}_{n,n} = +\widetilde{\mathcal{G}}_{\parallel}^n(0^+) + \widetilde{\mathcal{G}}_{\parallel}^{n+1}(0^-) \quad (9b)$$

$$\mathbf{M}_{n,n+1} = -\widetilde{\mathcal{G}}_{\parallel}^{n+1}(z_n - z_{n+1}) \quad (9c)$$

Writing down equation (6) equation for all N dielectric interfaces yields a $4N \times 4N$ system of linear equations, with triadiagonal 4×4 block form, relating the surface currents on all layers to the external fields due to sources in all regions:

$$\mathbf{M} \cdot \mathbf{s} = \mathbf{f} \quad (10)$$

³The 4×4 \mathbf{M} blocks here have 2×2 block structure:

$$\mathbf{M}_{n,n} = \sum_{r \in \{n, n+1\}} \frac{1}{2} \begin{pmatrix} -\frac{\omega \epsilon_r}{Z_0 q_{zr}} \mathbf{g}(k_r, \mathbf{q}) & 0 \\ 0 & -\frac{\omega \mu_r Z_0}{q_{zr}} \mathbf{g}(k_r, \mathbf{q}) \end{pmatrix} \quad (7)$$

$$\mathbf{M}_{n,n \pm 1} = \frac{1}{2} \begin{pmatrix} -\frac{\omega \epsilon_r}{Z_0 q_{zr}} \mathbf{g}(k_r, \mathbf{q}) & \mathbf{c}^{\pm} \\ -\mathbf{c}^{\pm} & -\frac{\omega \mu_r Z_0}{q_{zn}^*} \mathbf{g}(k_r, \mathbf{q}) \end{pmatrix} e^{iq_{zr}|z_n - z_{n \pm 1}|} \quad (8)$$

where I put $r \equiv \begin{cases} n, & \text{for } \mathbf{M}_{n,n-1} \\ n+1, & \text{for } \mathbf{M}_{n,n+1} \end{cases}$ and

$$\mathbf{g}(k; \mathbf{q}) = \mathbf{1} - \frac{\mathbf{q}\mathbf{q}^\dagger}{k^2}, \quad \mathbf{c}^{\pm} = \begin{pmatrix} 0 & \mp 1 \\ \pm 1 & 0 \end{pmatrix}$$

where \mathbf{M} is the $4N \times 4N$ block-tridiagonal matrix (9) and where the $4N$ -vectors \mathbf{s} , \mathbf{f} read

$$\mathbf{s} = \begin{pmatrix} \tilde{\mathcal{S}}_1 \\ \tilde{\mathcal{S}}_2 \\ \tilde{\mathcal{S}}_3 \\ \vdots \\ \tilde{\mathcal{S}}_N \end{pmatrix}, \quad \mathbf{f} = \begin{pmatrix} -\tilde{\mathcal{F}}_{1\parallel}(z_1) + \tilde{\mathcal{F}}_{2\parallel}(z_1) \\ -\tilde{\mathcal{F}}_{2\parallel}(z_2) + \tilde{\mathcal{F}}_{3\parallel}(z_2) \\ -\tilde{\mathcal{F}}_{3\parallel}(z_3) + \tilde{\mathcal{F}}_{4\parallel}(z_3) \\ \vdots \\ -\tilde{\mathcal{F}}_{N-1,\parallel}(z_{N-1}) + \tilde{\mathcal{F}}_{N\parallel}(z_{N-1}) \end{pmatrix}.$$

Solving (10) yields the induced surface currents on all layers in terms of the incident fields:

$$\mathbf{s} = \mathbf{W} \cdot \mathbf{f} \quad \text{where} \quad \mathbf{W} \equiv \mathbf{M}^{-1}$$

or, more explicitly,

$$\tilde{\mathcal{S}}_n = \sum_m W_{nm} \mathbf{f}_m \quad (11)$$

Surface currents induced by point sources

For DGF computations the incident fields arise from a single point source—say, a j -directed source in region s . Then the only nonzero length-4 blocks of the RHS vector in (10) are $\mathbf{f}_{s-1}, \mathbf{f}_s$ with components ($\ell = \{1, 2, 4, 5\}$)

$$\left(\mathbf{f}_{s-1}\right)_\ell = -\widetilde{\mathcal{G}}_{\ell j\parallel}^s(z_{s-1} - z_s), \quad \left(\mathbf{f}_s\right)_\ell = +\widetilde{\mathcal{G}}_{\ell j\parallel}^s(z_s - z_s) \quad (12)$$

and the surface currents on interface layer n are obtained by solving (11):

$$\begin{aligned} \tilde{\mathcal{S}}_n &= \mathbf{W}_{n,s-1} \mathbf{f}_{s-1} + \mathbf{W}_{n,s} \mathbf{f}_s \\ &= \sum_{p=0}^1 (-1)^{p+1} \mathbf{W}_{n,s-1+p} \cdot \widetilde{\mathcal{G}}_{\parallel,j}^s(z_s - z_{s-1+p}) \end{aligned} \quad (13)$$

Fields due to surface currents

Given the surface currents induced by a j -directed point source at \mathbf{x}_s , I evaluate the fields due to these currents to get DGF components. If the evaluation point \mathbf{x}_d lies in region d , then the fields receive contributions from the surface currents at z_{d-1} and z_d , propagated by the homogeneous DGF for region d :

$$\begin{aligned} \tilde{\mathcal{F}}(z_d) &= -\widetilde{\mathcal{G}}^d(z_d - z_{d-1}) \cdot \tilde{\mathcal{S}}_{d-1} + \widetilde{\mathcal{G}}^d(z_d - z_d) \cdot \tilde{\mathcal{S}}_d \\ &= \sum_{q=0}^1 (-1)^{q+1} \widetilde{\mathcal{G}}^d(z_d - z_{d+q-1}) \cdot \tilde{\mathcal{S}}_{d+q-1} \end{aligned}$$

(The minus sign in the first term arises because, in my convention, surface currents on the upper surface of a region contribute to the fields in that region with a minus sign). Inserting (13), the i component here—which is the ij component of the substrate DGF—is

$$\widetilde{\mathcal{G}}_{ij}^{\text{subs}}(z_D, z_S) \equiv \widetilde{\mathcal{F}}_i(z_D) = \sum_{p,q=0}^1 (-1)^{p+q} \widetilde{\mathcal{G}}_{i,\parallel}^d(z_D - z_{d-1+q}) \mathbf{W}_{d-1+q,s-1+p} \widetilde{\mathcal{G}}_{\parallel,j}^s(z_{s-1+p} - z_S)$$

Inverse-Fourier-transforming back to real space yields

$$\mathcal{G}^{\text{subs}}(\boldsymbol{\rho}_D, z_D; \boldsymbol{\rho}_S, z_S) = \int \frac{d^2 \mathbf{q}}{(2\pi)^2} \widetilde{\mathcal{G}}^{\text{subs}}(\mathbf{q}; z_D; z_S) e^{i\mathbf{q} \cdot (\boldsymbol{\rho}_D - \boldsymbol{\rho}_S)}. \quad (14)$$

Reduction to 1D integrals

We will evaluate the Fourier integrals (14) in polar coordinates $\mathbf{q} = (q_x, q_y) = (q \cos \theta_{\mathbf{q}}, q \sin \theta_{\mathbf{q}})$. Although $\widetilde{\mathcal{G}}^{\text{subs}}(\mathbf{q})$ has 36 Cartesian components, these may be expressed in terms of just 14 scalar functions of q_ρ times cosines and sines of $\theta_{\mathbf{q}}$:

$$\begin{aligned} \widetilde{\mathcal{G}}^{\text{EE}}(\mathbf{q}) &= \widetilde{g}^{\text{EE0}\parallel}(q) \begin{pmatrix} 1 & 0 & 0 \\ 0 & 1 & 0 \\ 0 & 0 & 0 \end{pmatrix} + \widetilde{g}^{\text{EE0}z}(q) \begin{pmatrix} 0 & 0 & 0 \\ 0 & 0 & 0 \\ 0 & 0 & 1 \end{pmatrix} \\ &\quad + \widetilde{g}^{\text{EE1A}}(q) \begin{pmatrix} 0 & 0 & \cos \theta_{\mathbf{q}} \\ 0 & 0 & \sin \theta_{\mathbf{q}} \\ 0 & 0 & 0 \end{pmatrix} + \widetilde{g}^{\text{EE1B}}(q) \begin{pmatrix} 0 & 0 & 0 \\ 0 & 0 & 0 \\ \cos \theta_{\mathbf{q}} & \sin \theta_{\mathbf{q}} & 0 \end{pmatrix} \\ &\quad + \widetilde{g}^{\text{EE2}}(q) \begin{pmatrix} \cos^2 \theta_{\mathbf{q}} & \cos \theta_{\mathbf{q}} \sin \theta_{\mathbf{q}} & 0 \\ \cos \theta_{\mathbf{q}} \sin \theta_{\mathbf{q}} & \sin^2 \theta_{\mathbf{q}} & 0 \\ 0 & 0 & 0 \end{pmatrix} \\ \widetilde{\mathcal{G}}^{\text{EM}}(\mathbf{q}) &= g^{\text{EM0}\parallel}(q) \begin{pmatrix} 0 & 1 & 0 \\ -1 & 0 & 0 \\ 0 & 0 & 0 \end{pmatrix} + g^{\text{EM2}}(q) \begin{pmatrix} \cos \theta_{\mathbf{q}} \sin \theta_{\mathbf{q}} & \sin^2 \theta_{\mathbf{q}} & 0 \\ -\cos^2 \theta_{\mathbf{q}} & -\cos \theta_{\mathbf{q}} \sin \theta_{\mathbf{q}} & 0 \\ 0 & 0 & 0 \end{pmatrix} \\ &\quad + g^{\text{EM1A}}(q) \begin{pmatrix} 0 & 0 & -\sin \theta_{\mathbf{q}} \\ 0 & 0 & +\cos \theta_{\mathbf{q}} \\ 0 & 0 & 1 \end{pmatrix} + g^{\text{EM1B}}(q) \begin{pmatrix} 0 & 0 & 0 \\ 0 & 0 & 0 \\ -\sin \theta_{\mathbf{q}} & \cos \theta_{\mathbf{q}} & 1 \end{pmatrix} \\ \mathcal{G}^{\text{EE}}(\boldsymbol{\rho}, z, z') &= [g^{\text{EE0}\parallel}(\boldsymbol{\rho}, z, z') + g^{\text{EE2A}}(\boldsymbol{\rho}, z, z')] \begin{pmatrix} 1 & 0 & 0 \\ 0 & 1 & 0 \\ 0 & 0 & 0 \end{pmatrix} + g^{\text{EE0}z}(\boldsymbol{\rho}, z, z') \begin{pmatrix} 0 & 0 & 0 \\ 0 & 0 & 0 \\ 0 & 0 & 1 \end{pmatrix} \\ &\quad + g^{\text{EE1A}}(\boldsymbol{\rho}, z, z') \begin{pmatrix} 0 & 0 & \cos \theta_{\boldsymbol{\rho}} \\ 0 & 0 & \sin \theta_{\boldsymbol{\rho}} \\ 0 & 0 & 0 \end{pmatrix} + g^{\text{EE1B}}(\boldsymbol{\rho}, z, z') \begin{pmatrix} 0 & 0 & 0 \\ 0 & 0 & 0 \\ \cos \theta_{\boldsymbol{\rho}} & \sin \theta_{\boldsymbol{\rho}} & 0 \end{pmatrix} \\ &\quad + g^{\text{EE2}}(\boldsymbol{\rho}, z, z') \begin{pmatrix} \cos^2 \theta_{\boldsymbol{\rho}} & \cos \theta_{\boldsymbol{\rho}} \sin \theta_{\boldsymbol{\rho}} & 0 \\ \cos \theta_{\boldsymbol{\rho}} \sin \theta_{\boldsymbol{\rho}} & \sin^2 \theta_{\boldsymbol{\rho}} & 0 \\ 0 & 0 & 0 \end{pmatrix} \end{aligned}$$

$$\frac{1}{2\pi} \int_0^{2\pi} e^{iq\rho \cos(\theta_q - \theta_\rho)} \begin{pmatrix} 1 \\ \cos \theta_q \\ \sin \theta_q \\ \cos^2 \theta_q \\ \cos \theta_q \sin \theta_q \\ \sin^2 \theta_q \end{pmatrix} d\theta_q = \begin{pmatrix} J_0(q\rho) \\ iJ_1(q\rho) \cos \theta_\rho \\ iJ_1(q\rho) \sin \theta_\rho \\ -J_2(q\rho) \cos^2 \theta_\rho + \frac{J_1(q\rho)}{q\rho} \\ -J_2(q\rho) \cos \theta_\rho \sin \theta_\rho \\ -J_2(q\rho) \sin^2 \theta_\rho + \frac{J_1(q\rho)}{q\rho} \end{pmatrix},$$

Figure 3: Table of integrals used to reduce 2D integrals over \mathbf{q} to 1D integrals over $|q|$.

$$\begin{aligned} g^{\text{EE}0\parallel}(\rho, z, z') &= \int_0^\infty \tilde{g}^{\text{EE}0\parallel}(q, z, z') J_0(q\rho) \frac{q dq}{2\pi} \\ g^{\text{EE}0z}(\rho, z, z') &= \int_0^\infty \tilde{g}^{\text{EE}0z}(q, z, z') J_0(q\rho) \frac{q dq}{2\pi} \\ g^{\text{EE}1\text{A}}(\rho, z, z') &= i \int_0^\infty \tilde{g}^{\text{EE}1\text{A}}(q, z, z') J_1(q\rho) \frac{q dq}{2\pi} \\ g^{\text{EE}1\text{B}}(\rho, z, z') &= i \int_0^\infty \tilde{g}^{\text{EE}1\text{B}}(q, z, z') J_1(q\rho) \frac{q dq}{2\pi} \\ g^{\text{EE}2\text{A}}(\rho, z, z') &= \int_0^\infty \tilde{g}^{\text{EE}2}(q, z, z') \frac{J_1(q\rho)}{q\rho} \frac{q dq}{2\pi} \\ g^{\text{EE}2\text{B}}(\rho, z, z') &= - \int_0^\infty \tilde{g}^{\text{EE}2}(q, z, z') J_2(q\rho) \frac{q dq}{2\pi} \end{aligned}$$

Evaluation of 1D integrals

$$\int_0^\infty \frac{q dq}{2\pi} f(q) = \sum_{r=1}^{\text{NL}+1} \int_{q_r^{\min}}^{q_r^{\max}} \frac{q dq}{2\pi} f(q)$$

$$(q_1^{\min}, q_1^{\max}) = (0, k_0)$$

$$(q_2^{\min}, q_2^{\max}) = (k_0, k_1)$$

$$\vdots = \vdots$$

$$(q_{\text{NL}}^{\min}, q_{\text{NL}}^{\max}) = (k_{\text{NL}-1}, k_{\text{NL}})$$

$$(q_{\text{NL}+1}^{\min}, q_{\text{NL}+1}^{\max}) = (k_{\text{NL}}, \infty)$$

Special case: DGF for sources above single layer

The simplest case is that in which we have only a single material interface, i.e. the geometry consists of two semi-infinite half-spaces that meet at $z = z_1$. Then the first of Equation (5) decouples into separate 2×2 systems for $\tilde{\mathbf{K}}$ and $\tilde{\mathbf{N}}$:

$$\underbrace{\left[-\frac{k_A Z_0 Z_A}{2q_{zA}} \mathbf{g}(k_A, \mathbf{q}) - \frac{k_1 Z_0 Z_1}{2q_{z1}} \mathbf{g}(k_1, \mathbf{q}) \right]}_{\mathbf{M}_K} \tilde{\mathbf{K}} = -\tilde{\mathbf{E}}_{\parallel 0}^{\text{ext}}(z_1)$$

$$\underbrace{\left[-\frac{k_A}{2Z_0 Z_A q_{zA}} \mathbf{g}(k_A, \mathbf{q}) - \frac{k_1}{2Z_0 Z_1 q_{z1}} \mathbf{g}(k_1, \mathbf{q}) \right]}_{\mathbf{M}_N} \tilde{\mathbf{N}} = -\tilde{\mathbf{H}}_{\parallel 0}^{\text{ext}}(z_1)$$

If the externally-sourced fields are produced by point electric and magnetic sources \mathbf{p}, \mathbf{m} at a point $\mathbf{x}_S = (\boldsymbol{\rho}_S, z_S)$ (where “S” stands for “source”) above the interface at z_1 , we may insert equation (21) for the RHS here and solve for $\tilde{\mathbf{K}}, \tilde{\mathbf{N}}$:

$$\tilde{\mathbf{K}} = + \frac{e^{-i\mathbf{q} \cdot \boldsymbol{\rho}_S + iq_{zA}|z_1 - z_S|}}{2\omega q_z} \left[ik_A Z_0 Z_A \mathbf{M}_K^{-1} \tilde{\mathbf{G}}_{\parallel}^{-}(\mathbf{k}_A, \mathbf{q}) \cdot \mathbf{p} + ik_A \mathbf{M}_K^{-1} \tilde{\mathbf{C}}_{\parallel}^{-}(\mathbf{k}_A, \mathbf{q}) \cdot \mathbf{m} \right]$$

$$\tilde{\mathbf{N}} = + \frac{e^{-i\mathbf{q} \cdot \boldsymbol{\rho}_S + iq_{zA}|z_1 - z_S|}}{2\omega q_z} \left[-ik_A \mathbf{M}_N^{-1} \tilde{\mathbf{C}}_{\parallel}^{-}(\mathbf{k}_A, \mathbf{q}) \cdot \mathbf{p} + \frac{ik_A}{Z_0 Z_A} \mathbf{M}_N^{-1} \tilde{\mathbf{G}}_{\parallel}^{-}(\mathbf{k}_A, \mathbf{q}) \cdot \mathbf{m} \right]$$

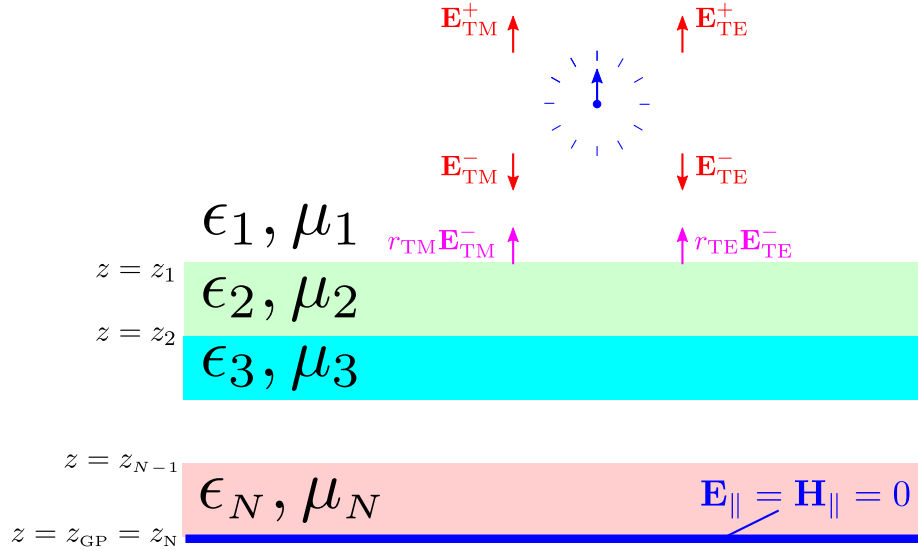


Figure 4: Plane-wave-decomposition strategy for handling multilayer substrate. The fields radiated by a point source (blue) above the substrate are decomposed as a superposition of upward- and downward-traveling plane waves, including both TE- and TM-polarized waves. The downward-traveling waves are reflected at the substrate surface with the usual polarization-dependent Fresnel reflection coefficients $r_{\text{TE,TM}}$, and the fields contributed by these reflected waves yield the correction to the free-space Green's function substrate.

2.2 Derivation of momentum-space DGF, take 2: Plane-wave (Fresnel) scattering picture)

One way of computing the substrate DGF correction, cartooned in Figure 4, is to think of the fields radiated by a point source above the substrate (blue) as a superposition of plane waves, including both TE- and TM-polarized plane waves (red). The upward-traveling waves radiated by the source ($\mathbf{E}_{\text{TE,TM}}^+$) simply radiate away to infinity and do not interact with the substrate, but the downward-traveling waves ($\mathbf{E}_{\text{TE,TM}}^-$) reflect from the substrate with polarization-dependent reflection coefficients $r_{\text{TE,TM}}$ to yield upward-traveling waves (purple) which constitute the substrate correction to the DGF.

An advantage of this approach is that it subsumes all details of the substrate into the reflection coefficients $r_{\text{TE,TM}}$. For simple substrates consisting of one or more homogeneous isotropic material layers these are easily computed in closed form, but the DGF approach here is more general and extends easily to cases involving anisotropic, birefringent, and/or chiral media (in which case the usual TE \rightarrow TE and TM \rightarrow TM reflections may be augmented by polarization-mixing terms) and even inhomogeneous substrates of arbitrary complexity for which

the reflection coefficients are known empirically.

2.2.1 Plane-wave decomposition of point-source fields

Note: In what follows, $\mathbf{q} = (q_x, q_y)$ is a *two-dimensional* vector and we have⁴

$$q_z \equiv \sqrt{k^2 - |\mathbf{q}|^2}, \quad \mathbf{q}^{3D} \equiv \begin{pmatrix} q_x \\ q_y \\ \pm q_z \end{pmatrix}, \quad \pm \equiv \begin{cases} +, & z \geq 0 \\ -, & z < 0 \end{cases}.$$

For arbitrary \mathbf{q} I define generalized⁵ transverse-electric and transverse-magnetic plane waves propagating with wavevector \mathbf{q}^{3D} :

$$\begin{aligned} \mathbf{E}_{\text{TE}}^\pm(\mathbf{x}; k; \mathbf{q}) &\equiv E_0 \mathbf{P}(\mathbf{q}) e^{i\mathbf{q} \cdot \boldsymbol{\rho} \pm i q_z z}, & \mathbf{H}_{\text{TE}}^\pm(\mathbf{x}; k; \mathbf{q}) &\equiv H_0 \bar{\mathbf{P}}(k, \mathbf{q}) e^{i\mathbf{q} \cdot \boldsymbol{\rho} \pm i q_z z}, \\ \mathbf{E}_{\text{TM}}^\pm(\mathbf{x}; k; \mathbf{q}) &\equiv -E_0 \bar{\mathbf{P}}(k, \mathbf{q}) e^{i\mathbf{q} \cdot \boldsymbol{\rho} \pm i q_z z}, & \mathbf{H}_{\text{TM}}^\pm(\mathbf{x}; k; \mathbf{q}) &\equiv H_0 \mathbf{P}(\mathbf{q}) e^{i\mathbf{q} \cdot \boldsymbol{\rho} \pm i q_z z}, \end{aligned}$$

$$\mathbf{x} = (\boldsymbol{\rho}, z), \quad E_0 \equiv 1 \text{ volt}/\mu\text{m}, \quad H_0 \equiv \frac{E_0}{Z_0}$$

where \mathbf{P} and $\bar{\mathbf{P}}$ are unit-magnitude polarization vectors with the properties that (1) both \mathbf{P} and $\bar{\mathbf{P}}$ are orthogonal to \mathbf{k}^{3D} , and (2) \mathbf{P} is orthogonal to $\hat{\mathbf{z}}$ (i.e. “transverse”).

$$\mathbf{P}(k, \mathbf{q}) \equiv \frac{1}{|\mathbf{q}|} \begin{pmatrix} -q_y \\ q_x \\ 0 \end{pmatrix}, \quad \bar{\mathbf{P}}(k, \mathbf{q}) \equiv \frac{1}{k} [\mathbf{q}^{3D} \times \mathbf{P}(\mathbf{q})] = \frac{1}{k|\mathbf{q}|} \begin{pmatrix} \mp q_x q_z \\ \mp q_y q_z \\ q_x^2 + q_y^2 \end{pmatrix}$$

The trick is now to notice that the columns of the 3×3 matrices in equation (4c,d) may be written as linear combinations of \mathbf{P} and $\bar{\mathbf{P}}$. For example, the leftmost column of $\tilde{\mathbf{G}}_\pm$ is

$$\begin{pmatrix} \tilde{G}_{xx} \\ \tilde{G}_{yx} \\ \tilde{G}_{zx} \end{pmatrix} = \frac{1}{k^2} \begin{pmatrix} k^2 - q_x^2 \\ -q_y q_x \\ \mp q_x q_z \end{pmatrix} = -\left(\frac{q_y}{|\mathbf{q}|}\right) \mathbf{P}(\mathbf{q}) \mp \left(\frac{q_x q_z}{k|\mathbf{q}|}\right) \bar{\mathbf{P}}(\mathbf{q}). \quad (15)$$

The fields of an $\hat{\mathbf{x}}$ -directed point electric dipole $\mathbf{p}_0 = p_0 \hat{\mathbf{x}}$ living at \mathbf{x}_S (for “source”), evaluated at point \mathbf{x}_D (for “destination”), then read

$$\mathbf{E}^E(\mathbf{x}_D; \{p_0 \hat{\mathbf{x}}, \mathbf{x}_S\}) = ikZ \begin{pmatrix} G_{xx} \\ G_{yx} \\ G_{zx} \end{pmatrix} (-i\omega p_0)$$

⁴More generally, the symbol \pm here should be understood as $\text{sign}(z_D - z_S)$, i.e. it is positive (negative) when the evaluation point lies above (below) the source point.

⁵These are “generalized” plane waves in the sense that q_z is imaginary for sufficiently large \mathbf{q} , in which case the waves are evanescent.

Insert (4b):

$$= (-i\omega p_0)(ikZ) \int \frac{d\mathbf{q}}{(2\pi)^2} \frac{i}{2q_z} \begin{pmatrix} \tilde{G}_{xx}^\pm \\ \tilde{G}_{yx}^\pm \\ \tilde{G}_{zx}^\pm \end{pmatrix} e^{i\mathbf{q} \cdot (\boldsymbol{\rho}_D - \boldsymbol{\rho}_S) + iq_z(z_D + z_S)}$$

Insert (15):

$$= \frac{k^2 p_0}{\epsilon E_0} \int \frac{d\mathbf{q}}{(2\pi)^2} \left\{ \underbrace{\left(-\frac{iq_y}{2q_z |\mathbf{q}|} \right)}_{C_{\text{TE}}^x} \mathbf{E}_{\text{TE}}^\pm(\mathbf{x}_D - \mathbf{x}_S; k; \mathbf{q}) + \underbrace{\left(\mp \frac{iq_x}{2k|\mathbf{q}|} \right)}_{C_{\text{TM}}^{x;\pm}} \mathbf{E}_{\text{TM}}^\pm(\mathbf{x}_D - \mathbf{x}_S; k; \mathbf{q}) \right\}$$

Continuing to play this game for point sources of all possible orientations and expressing the results in terms of the generalized plane waves we defined earlier then yields a full plane-wave decomposition of the fields of point electric dipoles oriented in all three Cartesian directions:

$$\mathbf{E}^E(\mathbf{x}_D; \{p_0 \hat{\mathbf{x}}, \mathbf{x}_S\}) = \left(\frac{k^2 p_0}{\epsilon_0 E_0} \right) \int \frac{d\mathbf{q}}{(2\pi)^2} \left\{ C_x^{\text{TE}}(\mathbf{q}) \mathbf{E}_{\text{TE}}^\pm(\mathbf{x}_D - \mathbf{x}_S; k; \mathbf{q}) + C_{x;\pm}^{\text{TM}}(\mathbf{q}) \mathbf{E}_{\text{TM}}^\pm(\mathbf{x}_D - \mathbf{x}_S; k; \mathbf{q}) \right\} \quad (16a)$$

$$\mathbf{E}^E(\mathbf{x}_D; \{p_0 \hat{\mathbf{y}}, \mathbf{x}_S\}) = \left(\frac{k^2 p_0}{\epsilon_0 E_0} \right) \int \frac{d\mathbf{q}}{(2\pi)^2} \left\{ C_y^{\text{TE}}(\mathbf{q}) \mathbf{E}_{\text{TE}}^\pm(\mathbf{x}_D - \mathbf{x}_S; k; \mathbf{q}) + C_{y;\pm}^{\text{TM}}(\mathbf{q}) \mathbf{E}_{\text{TM}}^\pm(\mathbf{x}_D - \mathbf{x}_S; k; \mathbf{q}) \right\} \quad (16b)$$

$$\mathbf{E}^E(\mathbf{x}_D; \{p_0 \hat{\mathbf{z}}, \mathbf{x}_S\}) = \left(\frac{k^2 p_0}{\epsilon_0 E_0} \right) \int \frac{d\mathbf{q}}{(2\pi)^2} \left\{ C_z^{\text{TE}}(\mathbf{q}) \mathbf{E}_{\text{TE}}^\pm(\mathbf{x}_D - \mathbf{x}_S; k; \mathbf{q}) + C_z^{\text{TM}}(\mathbf{q}) \mathbf{E}_{\text{TM}}^\pm(\mathbf{x}_D - \mathbf{x}_S; k; \mathbf{q}) \right\} \quad (16c)$$

where the scalar coefficients are

$$\begin{aligned} C_x^{\text{TE}} &= -\frac{iq_y}{2|\mathbf{q}|q_z} & C_{x;\pm}^{\text{TM}} &= \mp \frac{iq_x}{2k|\mathbf{q}|} \\ C_y^{\text{TE}} &= \frac{iq_x}{2|\mathbf{q}|q_z} & C_{y;\pm}^{\text{TM}} &= \mp \frac{iq_y}{2k|\mathbf{q}|} \\ C_z^{\text{TE}} &= 0 & C_z^{\text{TM}} &= \frac{i|\mathbf{q}|}{2kq_z}. \end{aligned}$$

or, in vector form,

$$\mathbf{C}^{\text{TE}}(k, \mathbf{q}) = -\frac{i}{2q_z} \mathbf{P}(k, \mathbf{q}), \quad \mathbf{C}^{\text{TM}}(k, \mathbf{q}) = -\frac{i}{2q_z} \bar{\mathbf{P}}(k, \mathbf{q}). \quad (17)$$

In these equations, the \pm sign is $+$ for evaluation points located above the source ($z > z_0$) and $-$ for evaluation points located below the source. In particular, assuming the source lies in the *upper* half-space ($z_0 > 0$), the fields impinging on a dielectric interface at $z = 0$ involve the $-$ sign.

The units of the source-strength prefactor are (C=charge, V=voltage, L=length)

$$\begin{aligned} \left[\left(\frac{k^2 p_0}{\epsilon_0 E_0} \right) \right] &= [k^2 p_0] [\epsilon_0]^{-1} [E_0]^{-1} \\ &= \frac{L^{-2} C \cdot L}{C V^{-1} L^{-1} V L^{-1}} \\ &= \text{length}. \end{aligned}$$

2.2.2 Plane-wave decomposition of DGFs

The point of the above decomposition is that each downward-traveling plane wave radiated by a point source above a substrate is reflected from the substrate with the polarization-dependent reflection coefficients $r_{\text{TE}, \text{TM}}(k, \mathbf{q})$ characteristic of the substrate, and thus the scattered fields are

$$\mathbf{E}^{\text{scat}, x}(\boldsymbol{\rho}, z) = \left(\frac{k^2 p_0}{\epsilon_0} \right) \int \frac{d\mathbf{q}}{(2\pi)^2} \left\{ r_{\text{TE}}(\mathbf{q}) C_x^{\text{TE}}(\mathbf{q}) \mathbf{P}(\mathbf{q}) + r_{\text{TM}}(\mathbf{q}) C_{x;-}^{\text{TM}}(\mathbf{q}) \bar{\mathbf{P}}(\mathbf{q}) \right\} e^{i\mathbf{q} \cdot \boldsymbol{\rho} + i q_z (z_D + z_S)} \quad (18a)$$

$$\mathbf{E}^{\text{scat}, y}(\boldsymbol{\rho}, z) = \left(\frac{k^2 p_0}{\epsilon_0} \right) \int \frac{d\mathbf{q}}{(2\pi)^2} \left\{ r_{\text{TE}}(\mathbf{q}) C_y^{\text{TE}}(\mathbf{q}) \mathbf{P}(\mathbf{q}) + r_{\text{TM}}(\mathbf{q}) C_{y;-}^{\text{TM}}(\mathbf{q}) \bar{\mathbf{P}}(\mathbf{q}) \right\} e^{i\mathbf{q} \cdot \boldsymbol{\rho} + i q_z (z_D + z_S)} \quad (18b)$$

$$\mathbf{E}^{\text{scat}, z}(\boldsymbol{\rho}, z) = \left(\frac{k^2 p_0}{\epsilon_0} \right) \int \frac{d\mathbf{q}}{(2\pi)^2} \left\{ r_{\text{TE}}(\mathbf{q}) C_z^{\text{TE}}(\mathbf{q}) \mathbf{P}(\mathbf{q}) + r_{\text{TM}}(\mathbf{q}) C_{z;-}^{\text{TM}}(\mathbf{q}) \bar{\mathbf{P}}(\mathbf{q}) \right\} e^{i\mathbf{q} \cdot \boldsymbol{\rho} + i q_z (z_D + z_S)} \quad (18c)$$

The substrate contribution to the electric-electric DGF is related to the scattered \mathbf{E} -field according to $\mathcal{G}^{\text{EE}} = \frac{1}{-i\omega p_0} \mathbf{E}^{\text{scat}}$, or

$$\mathcal{G}_{ij}^{\text{EE}}(\boldsymbol{\rho}, z_D, z_S) = ikZ \int \frac{d\mathbf{q}}{(2\pi)^2} \left\{ r_{\text{TE}}(\mathbf{q}) C_{\text{TE}}^j(\mathbf{q}) P_i(\mathbf{q}) + r_{\text{TM}}(\mathbf{q}) C_{\text{TM}}^{j;-}(\mathbf{q}) \bar{P}_i(\mathbf{q}) \right\} e^{i\mathbf{q} \cdot \boldsymbol{\rho} + i q_z (z_D + z_S)} \quad (19a)$$

or, using (17),

$$= \frac{kZ}{2} \int \frac{d\mathbf{q}}{(2\pi)^2 q_z} \left\{ r_{\text{TE}}(\mathbf{q}) P_i(\mathbf{q}) P_j(\mathbf{q}) + r_{\text{TM}}(\mathbf{q}) \bar{P}_i(\mathbf{q}) \bar{P}_j(\mathbf{q}) \right\} e^{i\mathbf{q} \cdot \boldsymbol{\rho} + i q_z (z_D + z_S)}. \quad (19b)$$

We get G^{ME} by making the replacements $\{P, \bar{P}\} \rightarrow \frac{1}{Z} \{\bar{P}, -P\}$:

$$\mathcal{G}_{ij}^{\text{ME}}(\boldsymbol{\rho}, z) = \frac{k}{2} \int \frac{d\mathbf{q}}{(2\pi)^2 q_z} \left\{ r_{\text{TE}}(\mathbf{q}) \bar{P}_i(\mathbf{q}) P_j(\mathbf{q}) - r_{\text{TM}}(\mathbf{q}) P_i(\mathbf{q}) \bar{P}_j(\mathbf{q}) \right\} e^{i\mathbf{q} \cdot \boldsymbol{\rho} + i q_z (z_D + z_S)} \quad (19c)$$

Fields of point-source currents

A point electric dipole of strength \mathbf{p}_0 at a point \mathbf{x}_0 corresponds to a volume electric current distribution of the form

$$\mathbf{J}(\mathbf{x}) = -\frac{\mathbf{p}_0}{i\omega} \delta(\mathbf{x} - \mathbf{x}_0),$$

or, in Fourier space,

$$\mathbf{J}(\mathbf{x}) = \int \frac{d\mathbf{q}}{(2\pi)^2} \tilde{\mathbf{J}}(\mathbf{q}) e^{i\mathbf{q} \cdot \mathbf{x}}$$

with

$$\begin{aligned} \tilde{\mathbf{J}}(\mathbf{q}) &= \int d\mathbf{x} \mathbf{J}(\mathbf{x}) e^{-i\mathbf{q} \cdot \mathbf{x}} \\ &= -\frac{\mathbf{p}_0}{i\omega} e^{-i\mathbf{q} \cdot \mathbf{x}_0}. \end{aligned}$$

Similarly, a point magnetic source of strength \mathbf{m}_0 corresponds to a magnetic current distribution with Fourier components

$$\tilde{\mathbf{M}}(\mathbf{q}) = -\frac{\mathbf{m}_0}{i\omega} e^{-i\mathbf{q} \cdot \mathbf{x}_0}.$$

The Fourier components of the fields $\mathcal{F} = \begin{pmatrix} \mathbf{E} \\ \mathbf{H} \end{pmatrix}$ at height z due to the sources $\mathcal{S} = \begin{pmatrix} \mathbf{K} \\ \mathbf{M} \end{pmatrix}$ at height z_0 read

$$\tilde{\mathcal{F}}(\mathbf{q}; z) = \tilde{\mathcal{G}}(\mathbf{q}, z - z_0) \cdot \tilde{\mathcal{S}}(\mathbf{q}, z_0) \quad (20)$$

or, from (4b)

$$\begin{aligned} \begin{pmatrix} \tilde{\mathbf{E}}(\mathbf{q}, z) \\ \tilde{\mathbf{H}}(\mathbf{q}, z) \end{pmatrix} &= \frac{i}{2q_z} \begin{pmatrix} ikZ\tilde{\mathbf{G}}^\pm & ik\tilde{\mathbf{C}}^\pm \\ -ik\tilde{\mathbf{C}}^\pm & \frac{ik}{Z}\tilde{\mathbf{G}}^\pm \end{pmatrix} \cdot \left(-\frac{1}{i\omega}\right) \begin{pmatrix} \mathbf{p}_0 \\ \mathbf{m}_0 \end{pmatrix} e^{-i\mathbf{q} \cdot \mathbf{x}_0 + iq_z|z - z_0|} \\ &= -\frac{1}{2\omega q_z} \begin{pmatrix} ikZ\tilde{\mathbf{G}}^\pm & ik\tilde{\mathbf{C}}^\pm \\ -ik\tilde{\mathbf{C}}^\pm & \frac{ik}{Z}\tilde{\mathbf{G}}^\pm \end{pmatrix} \begin{pmatrix} \mathbf{p}_0 \\ \mathbf{m}_0 \end{pmatrix} e^{-i\mathbf{q} \cdot \mathbf{x}_0 + iq_z|z - z_0|}. \quad (21) \end{aligned}$$

3 Plane-wave reflection coefficients for layered material substrates

3.1 Reflection coefficients for a single material interface

If the substrate consists of just a single semi-infinite material layer with relative material properties $\{\epsilon_r, \mu_r\}$ (and vacuum above), then the reflection coefficients in (18) are just the usual Fresnel coefficients:

$$r_{\text{TE}}(\omega, \mathbf{q}) \equiv \frac{\mu_r q_z - q'_z}{\mu q_z + q'_z}, \quad r_{\text{TM}}(\omega, \mathbf{q}) \equiv \frac{\epsilon_r q_z - q'_z}{\epsilon q_z + q'_z}$$

$$q_z = \sqrt{k_0^2 - |\mathbf{q}|^2}, \quad q'_z = \sqrt{\epsilon_r \mu_r k_0^2 - \mathbf{q}^2}, \quad k_0 \equiv \frac{\omega}{c}.$$

3.2 Reflection coefficients for multilayer substrates

4 Alternative approach to evaluating RWG integrals

$$\begin{aligned}
& \langle \mathbf{b}_\alpha | \mathcal{G}^{\text{subs}} | \mathbf{b}_\beta \rangle \\
&= \iint d\mathbf{x}_\alpha d\mathbf{x}_\beta b_{\alpha i}(\mathbf{x}_\alpha) \mathcal{G}_{ij}^{\text{subs}}(\mathbf{x}_\alpha, \mathbf{x}_\beta) b_{\beta j}(\mathbf{x}_\beta) \\
&= \iint d\mathbf{x}_\alpha d\mathbf{x}_\beta b_{\alpha i}(\mathbf{x}_\alpha) \left\{ \int \frac{d\mathbf{q}}{(2\pi)^2} \tilde{\mathcal{G}}_{ij}^{\text{subs}}(\mathbf{q}, z_\alpha, z_\beta) e^{i\mathbf{q} \cdot (\boldsymbol{\rho}_\alpha - \boldsymbol{\rho}_\beta)} \right\} b_{\beta j}(\mathbf{x}_\beta) \quad (22)
\end{aligned}$$

If both basis functions lie in the uppermost region, I have

$$\begin{aligned}
\tilde{\mathcal{G}}_{ij}^{\text{subs}}(\mathbf{q}, z_\alpha, z_\beta) &= \tilde{\mathcal{G}}_{i,\parallel}^1(\mathbf{q}, z_\alpha - z_1) \cdot \mathbf{W}_{1,1}(\mathbf{q}) \cdot \tilde{\mathcal{G}}_{\parallel,j}^1(\mathbf{q}, z_1 - z_\beta) \\
&= \tilde{\mathcal{G}}_{i,\parallel}^1(\mathbf{q}) \cdot \mathbf{W}_{1,1}(\mathbf{q}) \cdot \tilde{\mathcal{G}}_{\parallel,j}^1(\mathbf{q}) e^{iq_z(z_\alpha + z_\beta - 2z_1)}
\end{aligned}$$

$$\langle \mathbf{b}_\alpha | \mathcal{G}^{\text{subs}} | \mathbf{b}_\beta \rangle \quad (23)$$

$$= \int \frac{d\mathbf{q}}{(2\pi)^2} \left[\tilde{\mathcal{G}}_{i,\parallel}^1 \cdot \mathbf{W}_{1,1} \cdot \tilde{\mathcal{G}}_{\parallel,j}^1 e^{-2iq_z z_1} \right] \quad (24)$$

$$\times \underbrace{\left\{ \int d\mathbf{x}_\alpha b_{\alpha i}(\mathbf{x}_\alpha) e^{i(\mathbf{q} \cdot \mathbf{x}_\alpha + q_z z_\alpha)} \right\}}_{\tilde{b}_{\alpha i}(\mathbf{q} + q_z \hat{\mathbf{z}})} \times \underbrace{\left\{ \int d\mathbf{x}_\beta b_{\beta j}(\mathbf{x}_\beta) e^{i(-\mathbf{q} \cdot \mathbf{x}_\beta + q_z z_\beta)} \right\}}_{\tilde{b}_{\beta j}(-\mathbf{q} + q_z \hat{\mathbf{z}})} \quad (25)$$

The Fourier transforms of RWG source distributions can be evaluated in closed form, as I worked out previously in my memo on SCUFF-TRANSMISSION.⁶ The result is

$$\begin{aligned}
\tilde{b}(\mathbf{q}) &\equiv \int_{\text{sup } \mathbf{b}} \mathbf{b}_\alpha(\mathbf{x}) e^{i\mathbf{q} \cdot \mathbf{x}} d\mathbf{x} \\
&= \ell \sum_{\sigma \in \pm} \sigma e^{i\mathbf{q} \cdot \mathbf{Q}^\sigma} \left[f_u(\mathbf{q} \cdot \mathbf{A}^\sigma, \mathbf{q} \cdot \mathbf{B}) \mathbf{A}^\sigma + f_v(\mathbf{q} \cdot \mathbf{A}^\sigma, \mathbf{q} \cdot \mathbf{B}) \mathbf{B} \right]
\end{aligned}$$

where \mathbf{Q}^\pm are the source/sink vertices of the RWG function, $\mathbf{A}^\pm \equiv \mathbf{V}_1 - \mathbf{Q}^\pm$ and $\mathbf{B} = \mathbf{V}_2 - \mathbf{V}_1$ where $\mathbf{V}_{1,2}$ are the endpoints of the interior edge of the RWG function, ℓ is its length, and

$$\left\{ \begin{array}{c} f_u(x, y) \\ f_v(x, y) \end{array} \right\} \equiv \int_0^1 du \int_0^u dv \left\{ \begin{array}{c} u \\ v \end{array} \right\} e^{i(ux+vy)}.$$

⁶<http://homerreid.github.io/scuff-em-documentation/tex/scuff-transmission.pdf>

5 Evaluation of q integrals

$$\begin{aligned} I &= \int_0^\infty \mathcal{I}(q) dq \\ &= \underbrace{\int_0^a \mathcal{I}(q) dq}_{I^A} + \underbrace{\int_a^\infty \mathcal{I}(q) dq}_{I^B} \end{aligned}$$

$$z = at + ic \sin \pi t, \quad dz = (a + ic\pi \cos \pi t) dt, \quad 0 \leq t \leq 1$$

$$I^A = \int_0^a \mathcal{I}(q) dq = \int_{\mathcal{C}} \mathcal{I}(q) dq = \int_0^1 (a + i\pi \cos \pi t) \mathcal{I}(at + i \sin \pi t) dt$$

$$I^B = \sum_{n=1}^{\infty} I_n^B \quad I_n^B \equiv \int_{q_{n-1}}^{q_n} \mathcal{I}(q) dq$$

where $q_0 \equiv a$ and $\{q_1, \dots, q_N, \dots\}$ is an appropriately-chosen sequence of break points.